SPECIAL PROJECT FINAL REPORT

All the following mandatory information needs to be provided.

Project Title:	Exploit observations to constrain land cover, vegetation and hydrology processes for improved near-term climate predictions over land
Computer Project Account:	Spitales
Start Year - End Year:	2022 - 2024
Principal Investigator(s)	Andrea Alessandri
Affiliation/Address:	Institute of Atmospheric Sciences and Climate, National Research Council of Italy (ISAC-CNR) Via Gobetti 101 I-40129 Bologna, Italy
Other Researchers (Name/Affiliation):	Annalisa Cherchi (ISAC-CNR), Fransje van Oorschot (ISAC-CNR), Emanuele Di Carlo (ISAC-CNR), Marco Possega (ISAC-CNR), Vincenzo Senigalliesi (UNIBO, ISAC- CNR), Franco Catalano (ENEA), Etienne Tourigny (BSC), Pablo Ortega (BSC)

The following should cover the entire project duration.

Summary of project objectives

(10 lines max)

The objective of this special project is to exploit the latest available observational data over land to improve the representation of processes related to land cover, vegetation and hydrology that can positively contribute to skilful near-term climate predictions. Parameter-fitting and/or inverse modelling techniques will be employed to better constrain the land surface parameterizations to the available observations, followed by careful verification that will be first conducted off-line through ERA-5 forced land-only simulations. Finally, a set of decadal predictions with enhanced representation of land cover, vegetation and hydrology processes will be performed to assess the improvement of the predictions. With the remaining of resources, we'll preliminarily check the feasibility of actual forecasts with interactive vegetation by performing historical simulations with a post-CMIP6 configuration of EC-Earth3 that includes the vegetation dynamics (LPJ-Guess).

Summary of problems encountered

(If you encountered any problems of a more technical nature, please describe them here.)

We experienced major problems in the porting of the decadal prediction system based on the version 3 of the EC-Earth ESM on the Atos machine, mainly due to difficulties in adapting the Autosubmit workflow manager. It followed the decision by the EC-Earth prediction WG to not port this old system anymore but to concentrate on the development of a new decadal prediction system based on EC-Earth4 (to be expected on Atos after 2024). Consequently, we performed as much as possible the decadal hindcast sensitivity (DCPP-VEG) before cca was switched off. To this aim in 2022 we requested additional resources (16150000 SBUs) for SPITALES.
After cca switch off, with the migration of the ECMWF HPC system to the new Atos HPC2020 in Bologna, several libraries and packages were updated to more recent versions while the old versions, not being supported anymore, were removed. Consequently, we encountered several porting issues in particular related to the update to Python3 and the discontinued support to Python2, which required considerable effort in adapting and updating the scripts to configure and run EC-Earth.

Experience with the Special Project framework

(Please let us know about your experience with administrative aspects like the application procedure, progress reporting etc.)

No problems encountered with administrative aspects: we got all information and help needed.

Summary of results

(This section should comprise up to 10 pages, reflecting the complexity and duration of the project, and can be replaced by a short summary plus an existing scientific report on the project.)

i) The improved representation of land cover and vegetation processes

We used observational data of Leaf Area Index (LAI; from Copernicus Land Monitoring Service, CLMS), fraction of green vegetation cover (CLMS) and land cover (ESA-CCI) to introduce realistic variability representation in the model vegetation, and thereby enhance the variability in modeled land water and energy fluxes. Moreover, we developed an improved model parameterization of the effective vegetation cover based on the observational data.

We performed a comprehensive set of offline simulations (1980-2019 period, hourly ERA5 forcing; Hersbach et al., 2020) to evaluate the effects of the introduced vegetation variability on modeled evapotranspiration fluxes and soil moisture at the global scale by taking as reference global observational products (Hobeichi et al., 2021; Dorigo et al., 2017; Gruber et al., 2019).

Overall, our study demonstrated that the enhanced vegetation variability consistently improved the near-surface soil moisture and evapotranspiration variability, but the availability of reliable global observational data remains a limitation for complete understanding of the model response. To further explain the improvements found, we developed an interpretation framework for how the model development activates feedbacks between soil moisture, vegetation, and evaporation during vegetation water stress periods.

The outcomes of this analysis are discussed with details in the following peer-reviewed paper for the scientific community:

van Oorschot, F., van der Ent, R. J., Hrachowitz, M., Di Carlo, E., Catalano, F., Boussetta, S., Balsamo, G., and Alessandri, A., 2023: Interannual land cover and vegetation variability based on remote sensing data in the HTESSEL land surface model: implementation and effects on simulated water dynamics, Earth Syst. Dynam., 14, 1239–1259, https://doi.org/10.5194/esd-14-1239-2023

ii) The decadal prediction experiment with the improved vegetation representation in the EC-Earth ESM

The improved representation of land cover and vegetation described in the previous section has been integrated into the EC-Earth climate model. Leveraging this implementation, a new set of retrospective decadal predictions (DCPP-VEG) was performed, in which interannual variability in vegetation LAI and land cover/use was prescribed using observational datasets from CLMS and ESA-CCI. This experimental setup is designed to assess the upper bound of decadal climate predictability under perfect vegetation forcing conditions, thereby quantifying potential predictability. As a reference, the DCPP-CTRL experiment comprises previously conducted decadal hindcasts generated at the Barcelona Supercomputing Center. In DCPP-CTRL, LAI and land cover were prescribed from a prior EC-Earth simulation that employed interactive vegetation dynamics through online coupling with LPJ-GUESS. Both DCPP-VEG and DCPP-CTRL adhere to the CMIP6 DCPP-A experimental protocol, consisting of 10-member ensembles of 5-year forecasts, each initialized annually on 1 November from 1999 to 2014. The experimental design is summarised in Table 1.

	DCPP-CTRL	DCPP-VEG
Period	1999-2014	1999-2014
Start Dates	1 November	1 November
Members/Length(years)	10/5	10/5
Atmospheric IC	ERA-Interim	ERA-Interim
Ocean IC	ORAS4	ORAS4
LAI and Land Cover	prescribed and derived from an EC-Earth historical simulation coupled with the LPJ-GUESS	Prescribed interannual Varying LAI (CLMS) and land cover/use (ESA-CCI)
Effective vegetation cover parameterisation	Vegetation cover prescribed and derived from an EC-Earth historical simulation coupled with the LPJ-GUESS	Effective cover parameterisation as a function of LAI (K for each vegetation type)
Land IC	Offline ERA-Interim/Land type	Offline ERA5/Land type

Table 1: Experimental setup for DCPP-CTRL and DCPP-VEG.

Model skill was evaluated against ERA5 reanalysis data, with both model outputs and reanalysis fields interpolated onto a uniform 1° × 1° latitude-longitude grid. The near-surface (2-metre) air temperature (TAS) bias was analysed to assess the sensitivity of the climatological mean state to differences in vegetation representation.

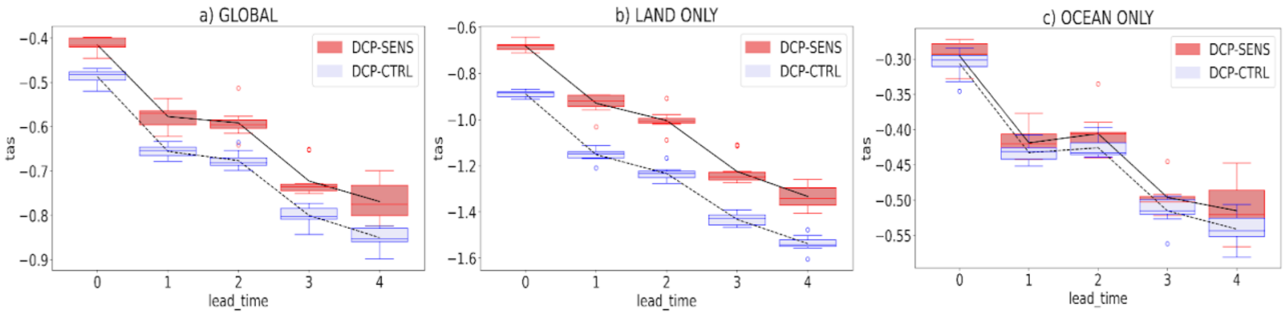

Figure 1: 2-meter temperature global average bias as a function of the lead year. a) Global average on all the grid points. b) Global average land points only. c) Global average ocean points only.

Figure 1 displays that the global TAS bias, is systematically reduced in the DCPP-VEG ensemble relative to DCPP-CTRL (Panel a), with a global mean reduction on the order of ~0.1 K. Panels b) and c) disaggregate the contributions from land and ocean regions, demonstrating that the bias reduction is predominantly confined to terrestrial areas, consistent with the targeted land-only modifications. On the other hand, oceanic biases remain largely unchanged in the two experiments.

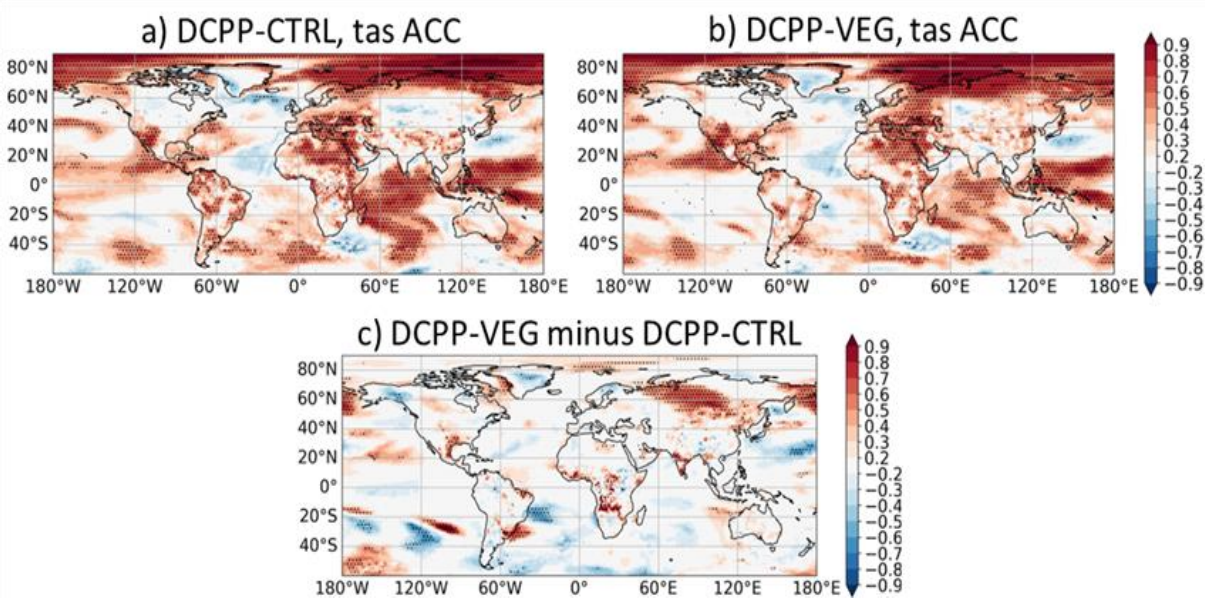

Figure 2: 2 m temperature ACC versus ERA5. a) DCPP-CTRL ACC, b) DCPP-VEG ACC, c) ACC difference, DCPP-VEG minus DCPP-CTRL. Dots represent statistically significant values, α=0.05.

Figure 2 illustrates the influence of vegetation representation on predictive skill, quantified using the anomaly correlation coefficient (ACC). Panels a) and b) show the ACC for DCPP-CTRL and DCPP-VEG, respectively. Spatial patterns of skill reveal moderate-to-high predictive capacity over high-latitude continental regions (excluding Greenland and parts of northern Canada), Central Europe, the southwestern United States, and portions of North Africa. Conversely, negative or near-zero skill is evident over Central Asia, mid-latitude North America, and Greenland. Over ocean basins, highest skill is found in the Mediterranean, Indian Ocean, and western tropical Pacific (aligned with the summer ITCZ), whereas the North Atlantic shows persistently low skill. Panel c) presents the ACC difference between the two experiments, highlighting regions of improved forecast performance in DCPP-VEG. Noteworthy, significant enhancements occur over the boreal forests of Central Asia—where DCPP-CTRL shows minimal skill—likely attributable to the inclusion of observational LAI and interannual land cover variability enabled by the new vegetation parameterization. Additional skill gains are evident over the Bering Sea and the deciduous forest regions of the southeastern United States. Improvements over the Bering Sea likely result from remote teleconnections with adjacent land areas, rather than direct effects of vegetation changes over oceanic regions.

This analysis will be discussed with more details in the following peer-reviewed paper for the scientific community that is currently under submission:

Di Carlo, E., et al., 2025: Enhancing Decadal Climate Predictability Through Improved Vegetation Cover Representation in EC-Earth, Under Submission

iii) Historical simulations with post-CMIP6 configuration of EC-Earth

We completed the historical simulation of EC-Earth3 that includes the latest modeling developments in a post-CMIP6 configuration (hereinafter EC-Earth3-ESM-1) for the period 1850-2014, following the CMIP6 protocol (Eyring et al 2016). Among other developments, the EC-Earth3-ESM-1 includes updated representation of vegetation [see section (i) above] and its interactive dynamics (LPJGuess; Nord et al., 2021), emission driven carbon cycle closure and the coupling with an ice sheet model. The historical simulation is started at year 1850 after a pre-industrial simulation of about 500 years produced at SMHI, and the initial conditions for the vegetation have been provided by Lund University and produced with LPJGuess offline and with boundary conditions taken from the pre-industrial control simulation. The transient results for the global land integrals of the total vegetation carbon pool (cveg; upper panel), of the soil carbon pool (csoil; middle panel) and of the total land carbon pool (cland; lower panel) are provided below (Figure 3).

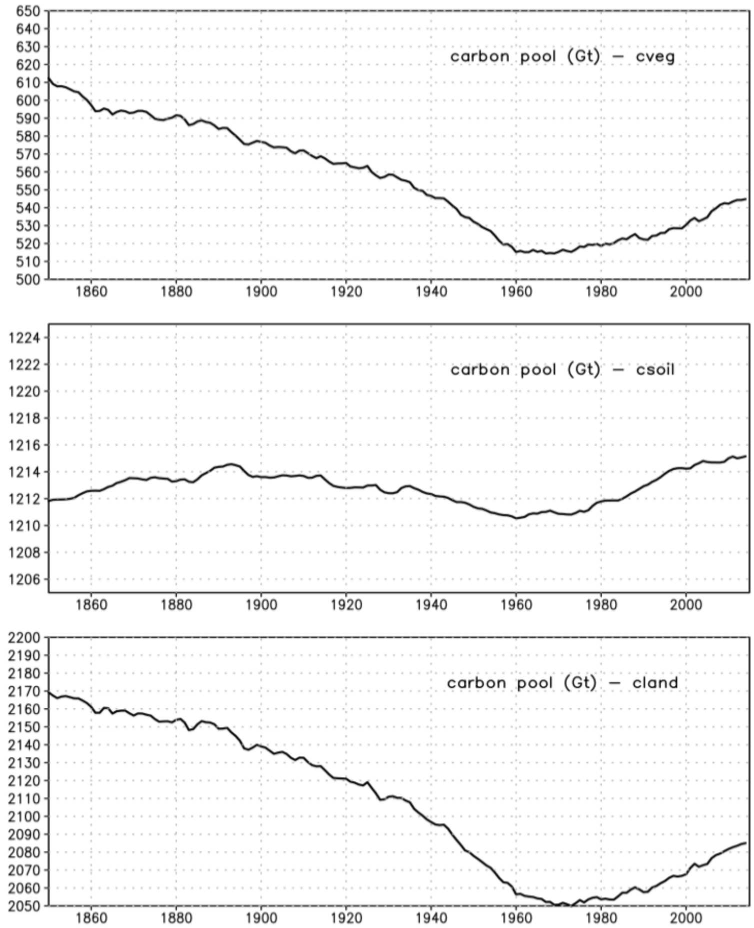

Figure 3: Time series of the total vegetation carbon pool (cveg; upper panel), of the soil carbon pool (csoil; middle panel) and total land carbon (cland=cveg+csoil; lower panel) integrated over global land areas.

Soil moisture persistence analysis – comparison with EC-Earth CMIP6 configurations

An analysis of the new post-CMIP6 historical simulation has been performed also comparing with previous historical runs delivered under CMIP6, i.e. the EC-Earth3 standard GCM configuration (EC-Earth3-GCM; consisting of the atmosphere model IFS, the land surface model HTESSEL with no vegetation dynamics, and the ocean model NEMO3.6 with the sea ice module LIM3; Doescher et al 2022) and the EC-Earth3-CC (configuration that includes a description of the carbon cycle and with representation of vegetation dynamics, and CO2 exchange with the land and ocean biogeochemistry; Doescher et al 2022). The main focus of this analysis has been on the representation of hydrological cycle processes—particularly soil moisture—and on drought persistence and trends that are of relevance for predictability, and with particular attention on water limited regions such as Mediterranean climate zones.

Standardized drought indices such as the Standardized Precipitation Index (SPI), the Standardized Soil Moisture Index (SSI), and the Standardized Runoff Index (SRI) have been computed annually using a non-parametric method (Hao et al. 2014). These indices were used to characterize key properties of soil moisture, including its climatology, long-term trends, and persistence that are compared across regions and time periods, and to identify significant drying and wetting patterns. In this regard, Figure 4 shows linear trends in the Standardized Soil Moisture Index (SSI) relative to the period 1980–2014 for the three configurations of the EC-Earth3 model. Negative trends (red) indicate increasing soil dryness, while positive trends (blue) indicate increasing wetness.

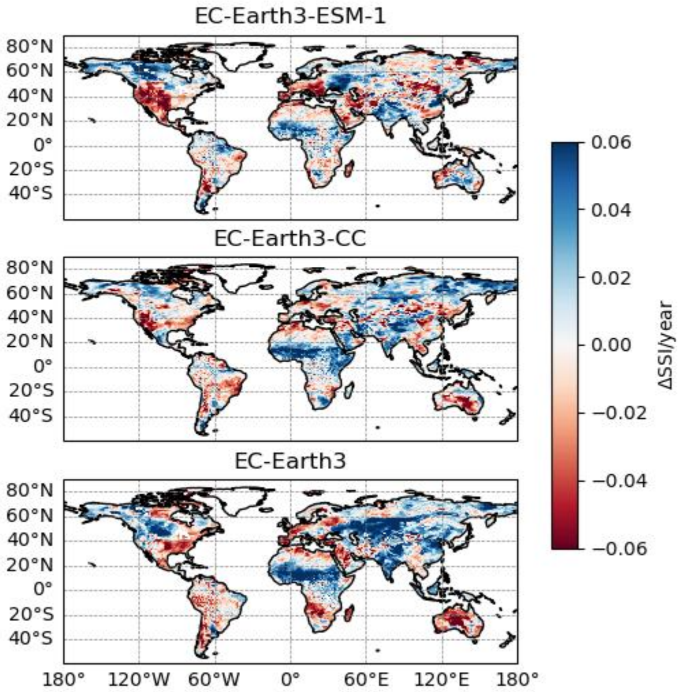

Figure 4: Pattern of SSI trends for 3 configurations of EC-Earth3 model, considering period 1980-2014.

In North America, the EC-Earth3-ESM-1 simulation shows a pronounced contrast between drying trends across much of the United States and wetting trends in the high-latitude regions. While similar features are partially captured by EC-Earth3-CC and EC-Earth3-GCM, they appear with lower intensity and less spatial coherence. Marked differences also emerge over Europe, where the post-CMIP6 configuration identifies the strongest drying trend, which is largely absent or weaker in the other two versions. Over the Sahel, EC-Earth3-ESM-1 shows a substantially reduced wetting signal compared to the more pronounced wetting seen in the simpler model configurations. Similarly, across much of Asia, the wetting trends are less intense in the ESM-1 version, particularly over South and Southeast Asia. In Australia, the discrepancies are especially relevant: EC-Earth3-ESM-1 simulates a general wetting trend in regions where the CMIP6 models instead show clear drying. Notably, the ESM-1 version also produces the most intense and spatially extensive drying trends globally. This could reflect the influence of its enhanced process representation—such as interactive vegetation dynamics, a fully coupled carbon cycle, and cryosphere feedbacks—which may amplify land–atmosphere interactions and lead to stronger hydroclimatic signal that could potentially contribute to predictability.

A dedicated component of the study has addressed the persistence of agricultural drought, quantified via the autocorrelation of the Standardized Soil Moisture Index (SSI) at different time lags. A specific focus of this analysis was placed on the Mediterranean region, where the spatial patterns of drought persistence were examined at various time lags for the three EC-Earth3 configurations over the period 1980–2014 (Figure 5). Distinct areas, such as the Balkans, Turkey, and the interior of the Iberian Peninsula, exhibit high SSI autocorrelation values (up to 0.6) even at long lags—beyond the annual scale—consistently across all three model versions. These regions indicate persistent soil moisture deficits during the analyzed period. Despite these commonalities, differences among the EC-Earth3 configurations become more evident at longer lags.

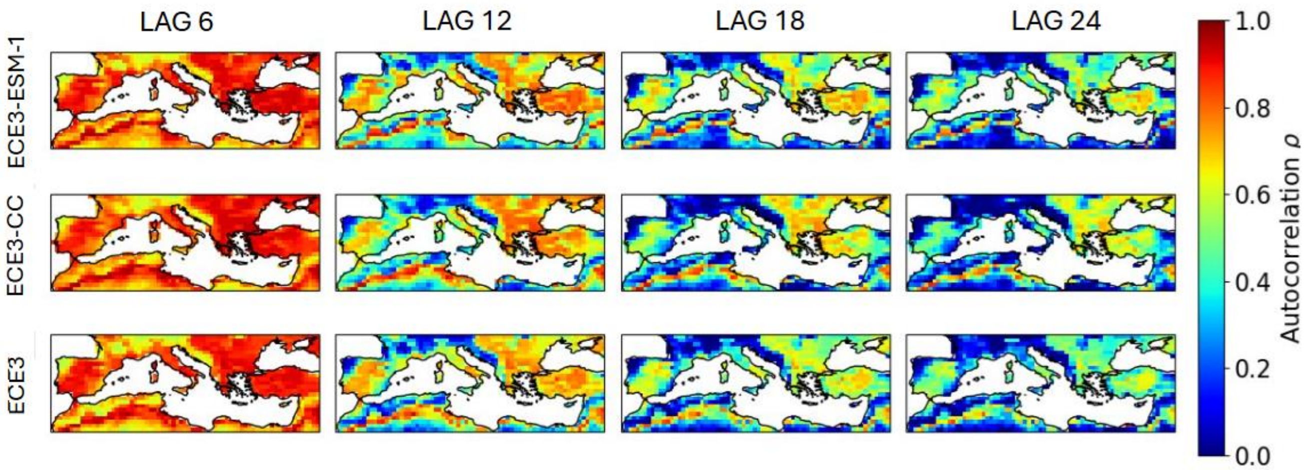

Figure 5: Pattern of drought persistence (SSI autocorrelation) at increasing lags for 3 configurations of EC-Earth3 model, considering period 1980-2014 over Mediterranean region [10°W - 40°E, 30°N - 48°N].

Figure 6 displays the average SSI autocorrelation over the Mediterranean domain as a function of time lag.

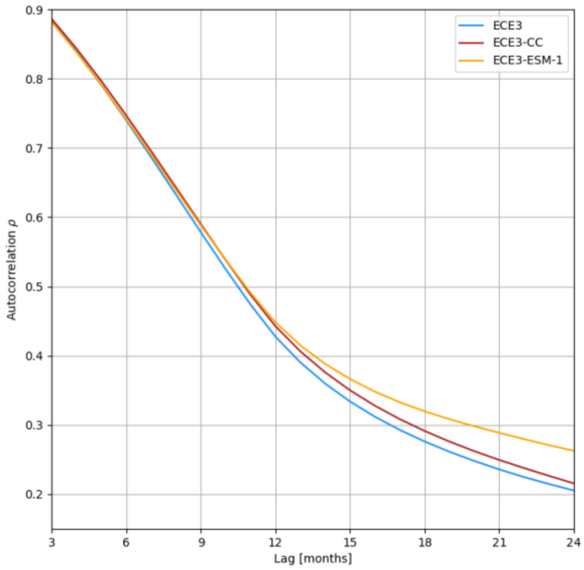

Figure 6: Lag-evolution of drought persistence (SSI autocorrelation) during 1980 – 2014 period for 3 configurations of EC-Earth3 model, averaged over Mediterranean region [10°W - 40°E, 30°N - 48°N].

While the three configurations show similar autocorrelation values at short lags (less than 6 months), differences emerge as the lag increases. EC-Earth3-CC shows a slight increase in SSI autocorrelation compared to EC-Earth3-GCM, whereas EC-Earth3-ESM-1 exhibits a more pronounced increase, particularly at longer lags. This confirms the EC-Earth3-ESM-1 tendency to simulate stronger predictive signal, in the form of drought persistence, compared to the CMIP6 configurations, that appears to be at least in part related to the enhanced representation of vegetation dynamics and its coupling with soil moisture.

This analysis will be discussed with more details in the following peer-reviewed paper for the scientific community that is currently in preparation (Possega et al. 2025):

Possega, M., et al., 2025: Analysis of soil modulation of drought persistence in Mediterranean for post-CMIP6 models, In Preparation

References:

Di Carlo, E., et al., 2025: Enhancing Decadal Climate Predictability Through Improved Vegetation Cover Representation in EC-Earth, Under Submission

Dorigo, W. et al. 2017: ESA CCI Soil Moisture for improved Earth system understanding: State-of-the art and future directions, Remote Sensing of Environment, 203, 185–215, https://doi.org/10.1016/j.rse.2017.07.001

Döscher, R., Acosta, M., Alessandri, A., Anthoni, P., Arsouze, T., Bergman, T., Bernardello, and co-authors, 2022: The EC-Earth3 Earth system model for the Coupled Model Intercomparison Project 6, Geosci. Model Dev., 15, 2973–3020, https://doi.org/10.5194/gmd-15-2973-2022

Eyring, V., Bony, S., Meehl, G. A., Senior, C. A., Stevens, B., Stouffer, R. J., and Taylor, K. E., 2016: Overview of the Coupled Model Intercomparison Project Phase 6 (CMIP6) experimental design and organization, Geosci. Model Dev., 9, 1937–1958, https://doi.org/10.5194/gmd-9-1937-2016.

Hao, Z., & AghaKouchak, A., 2014: A nonparametric multivariate multi-index drought monitoring framework. Journal of Hydrometeorology, 15(1), 89-101. https://doi.org/10.1175/JHM-D-12-0160.1

Hersbach, H, Bell, B, Berrisford, P, et al., 2020: The ERA5 global reanalysis. Q J R Meteorol Soc; 146: 1999– 2049. https://doi.org/10.1002/qj.3803https://doi.org/10.1002/qj.3803

Hobeichi, S., Abramowitz, G., and Evans, J. P., 2021: Robust historical evapotranspiration trends across climate regimes, Hydrol. Earth Syst. Sci., 25, 3855–3874, https://doi.org/10.5194/hess-25-3855-2021

Gruber, A., Scanlon, T., Van Der Schalie, R., Wagner, W., and Dorigo, W., 2019: Evolution of the ESA CCI Soil Moisture climate data records and their underlying merging methodology, Earth System Science Data, 11, 717–739, https://doi.org/10.5194/essd-11-717-2019

Nord, J., Anthoni, P., Gregor, K., Gustafson, A., Hantson, S., Lindeskog, M., Meyer, B., Miller, P., Nieradzik, L., Olin, S., Papastefanou, P., Smith, B., Tang, J., Wårlind, D., & and past LPJ-GUESS contributors. (2021). LPJ-GUESS Release v4.1.1 model code (4.1.1). Zenodo. https://doi.org/10.5281/zenodo.8065737

Possega, M., et al., 2025: Analysis of soil modulation of drought persistence in Mediterranean for post-CMIP6 models, In Preparation

van Oorschot, F., van der Ent, R. J., Hrachowitz, M., Di Carlo, E., Catalano, F., Boussetta, S., Balsamo, G., and Alessandri, A., 2023: Interannual land cover and vegetation variability based on remote sensing data in the HTESSEL land surface model: implementation and effects on simulated water dynamics, Earth Syst. Dynam., 14, 1239–1259, https://doi.org/10.5194/esd-14-1239-2023

List of publications/reports from the project with complete references

van Oorschot, F., Hrachowitz, M., Viering, T., Alessandri, A., and. van der Ent, R., 2024: Global patterns in vegetation accessible subsurface water storage emerge from spatially varying importance of individual drivers, ERL, 19, 124018, https://doi.org/10.1088/1748-9326/ad8805

van Oorschot, F., van der Ent, Alessandri, A., and Hrachowitz, M., 2024: Influence of irrigation on root zone storage capacity estimation, HESS, 28, 2313–2328, https://doi.org/10.5194/hess-28-2313-2024

van Oorschot, F., van der Ent, R. J., Hrachowitz, M., Di Carlo, E., Catalano, F., Boussetta, S., Balsamo, G., and Alessandri, A., 2023: Interannual land cover and vegetation variability based on remote sensing data in the HTESSEL land surface model: implementation and effects on simulated water dynamics, Earth Syst. Dynam., 14, 1239–1259, https://doi.org/10.5194/esd-14-1239-2023

Di Carlo, E., et al., 2025: Enhancing Decadal Climate Predictability Through Improved Vegetation Cover Representation in EC-Earth, Under Submission

Possega, M., et al., 2025: Analysis of soil modulation of drought persistence in Mediterranean for post-CMIP6 models, In Preparation

Future plans

(Please let us know of any imminent plans regarding a continuation of this research activity, in particular if they are linked to another/new Special Project.)

The beneficial effects of better constrained land-cover and vegetation processes shown in this special project motivates a new special project [SPITALES - 2025-2027] aimed at developing a more realistic representation of hydrology/groundwater and its coupling with vegetation in EC-Earth.